Available online at www.eccomasproceedia.org
Eccomas Proceedia COMPDYN (2019) 1933-1945

ECCOMAS
Proceedia

COMPDYN 2019
7th ECCOMAS Thematic Conference on
Computational Methods in Structural Dynamics and Earthquake Engineering
M. Papadrakakis, M. Fragiadakis (eds.)
Crete, Greece, 24–26 June 2019

PILE-HEAD KINEMATIC BENDING OF FIXED-HEAD LONG PILES IN HOMOGENEOUS AND LAYERED SOILS CONSIDERING PILE AND SOIL MATERIAL NONLINEARITIES IN CASE OF MODERATE TO STRONG EARTHQUAKE MOTIONS

S. Stacul[1], A. Franceschi[1], and N. Squeglia[1]

[1] Department of Civil and Industrial Engineering, University of Pisa
Largo Lucio Lazzarino, 1, 56122, Pisa, Italy
e-mail: stefano.stacul@for.unipi.it, anna.franceschi17@gmail.com, squeglia@ing.unipi.it

Abstract

The knowledge of fixed-head long piles response mechanism under harmonic excitations and earthquakes significantly increased in the last decades. Most of seismic codes suggest considering kinematic interaction for specific structures, in layered soil with high stiffness contrast and in case of high seismic input. More recently has been shown the importance of kinematic interaction in the design of concrete piles, especially when embedded in soft soil. Above all, the existence of a maximum allowable diameter ruled by kinematic interaction, affecting detrimentally the design in seismic conditions, has been identified. These findings are based on the main assumption that the soil is a linear viscoelastic material and the concrete remain in the uncracked stage. Here a recently developed BEM based code, called KIN SP, is used to provide new insights on pile-soil interaction during earthquakes. KIN SP models the nonlinear soil behavior with the Ramberg-Osgood law and the influence of concrete cracking is accounted, allowing to consider the cyclic variation of the pile flexural rigidity. The influence of pile and soil material nonlinearities in the assessment of pile-head kinematic bending both in homogenous and in layered soils will be discussed in case of moderate to strong earthquake motions. KIN SP results will be compared with commonly used simplified formulations available in literature. The results obtained show that material nonlinearities are relevant in the assessment of pile-head kinematic bending. The use of simplified solutions may lead to overestimate or underestimate pile-head bending moment.

Keywords: kinematic interaction, pile-head kinematic bending, soil-structure interaction, KIN SP, seismic response analysis, nonlinear kinematic analysis.

ISSN:2623-3347
Peer-review under responsibility of the organizing committee of COMPDYN 2019.
doi: 10.7712/120119.7047.19598

1 INTRODUCTION

1.1 Literature overview

Seismically induced kinematic bending of piles has been studied in pioneering contributions by [1, 2, 3, 4, 5, 6]. Many authors have proposed simplified methods to assess the kinematic bending at the interface of two-layered soil and at the pile-head [2, 5, 7, 8, 9] using beam on dynamic Winkler foundation models. On the other hand, others proposed to study the kinematic response of a single pile via the boundary element method (BEM) [6] and the finite element method [10, 11, 12, 13].

Pile-head kinematic bending in a homogenous soil or in a two-layered soil in which the interface is located at a depth higher than a critical one ($h_{c1} = 1.25D(E_p/E_1)^{0.25}$) [11] can be assumed equal to that inferred by the Equation (1) [11, 14].

$$M_{h,KIN} = E_p I_p \cdot \left(\frac{1}{R}\right)_s = E_p \frac{\pi D^4}{64} \frac{a_s}{V_{s1}^2} \tag{1}$$

Where: E_p is the pile elastic modulus, I_p the area moment of inertia of the pile section, $(1/R)_s$ the soil curvature at the pile-head, D the pile diameter, a_s the free-field peak ground acceleration, while V_{s1} and E_1 are the shear wave velocity and the elastic modulus of the upper soil layer, respectively.

In the case of fixed-head long pile embedded in nonhomogenous soil, Di Laora and Rovithis (2014) [15] suggested to evaluate the pile-head kinematic bending, once assessed an effective soil curvature, $(1/R)_{s,eff}$, using the Equation (2) or the Equation (3).

$$M_{h,KIN} = E_p I_p \cdot \left(\frac{1}{R}\right)_{s,eff} = E_p I_p \cdot \frac{a_s \rho_s}{G_s\left(z_{eff}\right)} \tag{2}$$

$$M_{h,KIN} = E_p I_p \cdot \left(\frac{1}{R}\right)_{s,eff} = E_p I_p \cdot \frac{\gamma_s\left(z_{eff}\right)}{z_{eff}} \tag{3}$$

Where: z_{eff} stands for an effective depth of soil contributing to kinematic pile-head bending, $G_s(z_{eff})$ and $\gamma_s(z_{eff})$ are the corresponding shear modulus and shear strain, respectively. The effective soil curvature represents an average soil curvature along z_{eff}, reflecting the physics of the interaction mechanism. $G_s(z_{eff})$ represents the shear modulus of an equivalent homogeneous soil deposit leading to a pile-head bending as in the inhomogeneous case.

In the study of Di Laora and Rovithis (2014) [15] a continuously inhomogeneous viscoelastic soil deposit lying on a rigid base was studied, in which the shear modulus increased following a generalized power law function (Equation 4).

$$G(z) = G_{sD} \cdot \left[a + (1-a) \cdot \frac{z}{D}\right]^n \tag{4}$$

Where: G_{sD} is the shear modulus at the depth of one pile diameter, $a=(G_{s0}/G_{sD})^{1/n}$ and n are dimensionless inhomogeneity factors and G_{s0} is the shear modulus at the ground surface. An iterative procedure has been proposed in [15] to evaluate z_{eff}, which was found to be approximately equal to one-half the pile active length.

In [11, 16, 17] the existence of a range of admissible pile diameters able to resist to combined inertial and kinematic bending at the pile-head was demonstrated. One of the main findings in these works was the fact that the design limitation related to a maximum allowable pile diameter is achieved only in case of homogeneous and very soft inhomogeneous soils. The range of admissible pile diameters can be estimated once defined the pile section capacity

and the pile-head inertial bending as shown in [11, 16, 18]. These findings have been obtained neglecting both the soil and pile nonlinearities. In this paper the importance of considering both soil and pile nonlinear behaviour in the assessment of pile-head kinematic bending of fixed-head long piles in homogeneous and layered soils is studied. Herein kinematic analyses are carried out using a recently proposed code, called KIN SP (Stacul and Squeglia 2018 [19] Stacul et al. 2019 [18]). KIN SP has been improved to consider the effects due to reinforced concrete cracking.

2 BEM-BASED KINEMATIC ANALYSIS OF SINGLE PILE

Single pile kinematic analysis with the code KIN SP is performed using as input the seismic response analysis (SRA) results obtained with the code ONDA [20, 21, 22]. SRAs with ONDA are carried out in the time domain and the nonlinear soil behaviour is accounted via the Ramberg-Osgood [23] constitutive model. KIN SP and ONDA are completely merged to provide a stand-alone analysis tool. Detailed description of the main assumptions in KIN SP are presented in [19, 24, 25]. In [18] KIN SP has been enhanced to consider the reinforced concrete model proposed by Andreotti and Lai (2017) [26]. The latter permits to model the dynamic response of a reinforced concrete pile. In [26] the pre-yielding behaviour is modelled using three rules. The first rule defines the loading/unloading response in the uncracked stage with the intact flexural rigidity. The second rule defines the first loading path in the cracked stage, thus a cracked flexural rigidity, $(E_pI_p)_{cr} = |(M_y-M_{max})/(\psi_y-\psi_{max})|$ is assigned to the section. Once the cracking moment (M_{cr}) is exceeded, the section is marked as cracked and the maximum moment in the section (M_{max}) is updated. Where ψ_y and M_y are the section curvature and the bending moment at yielding, respectively. The third rule models the unloading/reloading path in the cracked stage. In the latter case a secant flexural rigidity, $(E_pI_p)_{se} = |M_{max}/\psi_{max}|$ is assigned. The post-yielding phase described in [26] has not been considered.

3 LINEAR ELASTIC ANALYSIS

3.1 Reference soil deposit and pile properties for linear analyses

The kinematic analyses using KIN SP have been realized on three simplified soil profiles with a total thickness of 30 m and overlying a bedrock with a shear wave velocity equal to 800 m/s and a unit weight of 22 kN/m^3. These profiles (Figure 1) have a uniform, a linear and a parabolic shear modulus distribution with depth and are characterized by the same $V_{s,30}$ (120 m/s), while the soil unit weight and the Poisson's ratio were considered equal to 19 kN/m^3 and 0.4, respectively.

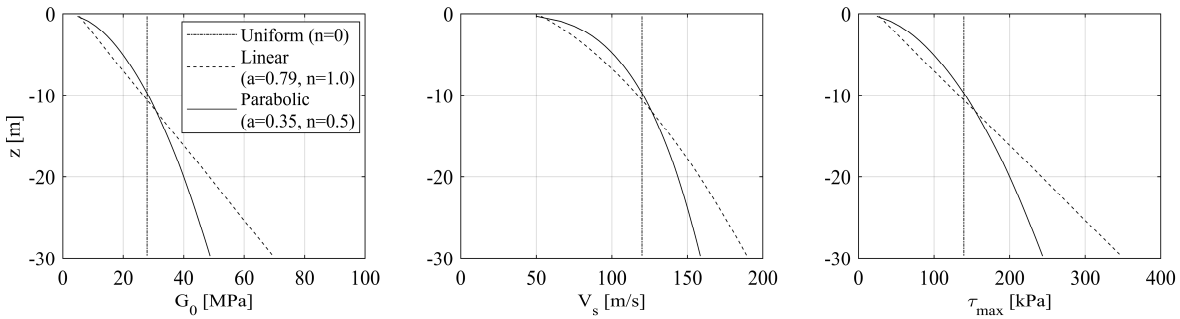

Figure 1: Shear modulus at small-strain (G_0), Shear wave velocity at small-strain (V_s) and shear strength (τ_{max}) profiles of the 3 soil deposits considered for the kinematic interaction analyses.

The parameter $V_{s,30}$ is an average shear wave velocity of the first 30 m. The resulting profiles can be classified as subsoil type D, according to EN-1998-1 (2005) [27]. In Table 1 are reported the parameters G_{s0}, G_{sD}, a and n to reproduce the shear modulus distributions with depth in Figure 1 according to the Equation 4 (Di Laora and Rovithis 2014 [15]). In the same table are shown the values of z_{eff} and $G_s(z_{eff})$ computed following Di Laora and Rovthis (2014) [15].

Profile	G_{s0} [MPa]	G_{sD} [MPa]	a [-]	n [-]	z_{eff} [m]	$G_s(z_{eff})$ [MPa]
Uniform	27.89	27.89	1.0	1.0	1.70	27.89
Parabolic	4.84	8.23	0.35	0.50	1.947	12.94
Linear	4.84	6.149	0.79	1.0	2.116	9.45

Table 1: Properties of the subsoil profiles adopted in this study (Equation 4).

Linear-elastic free-field response analyses have been performed with ONDA in time domain considering a soil damping β_s equal to 10%. The pile had the following properties: diameter D = 0.60m, length L = 20 m and elastic modulus E_p = 30 GPa. The pile-head was considered fixed against the rotation.

The acceleration time histories (Table 2) used in this work (identified by the codes: STU, NCB) have been selected from the Italian Accelerometric Archive [28], scaled to a value of a_r equal to 0.35g (for linear analysis) and applied to the base of the soil deposit model. These two input motions were considered due to their differences (Table 2, Figure 2) in terms of magnitude (M_W) frequency content, significant duration, mean period (T_m) and predominant period (T_p) [29].

Code	Station	Event ID	Orient.	M_W	Duration	T_m [s]	T_p [s]
NCB	Nocera U.	IT-1997-0091	E-W	5.4	3.16s	0.167	0.117
STU	Sturno	IT-1980-0012	E-W	6.9	36.45s	0.927	0.208

Table 2: Input motions properties.

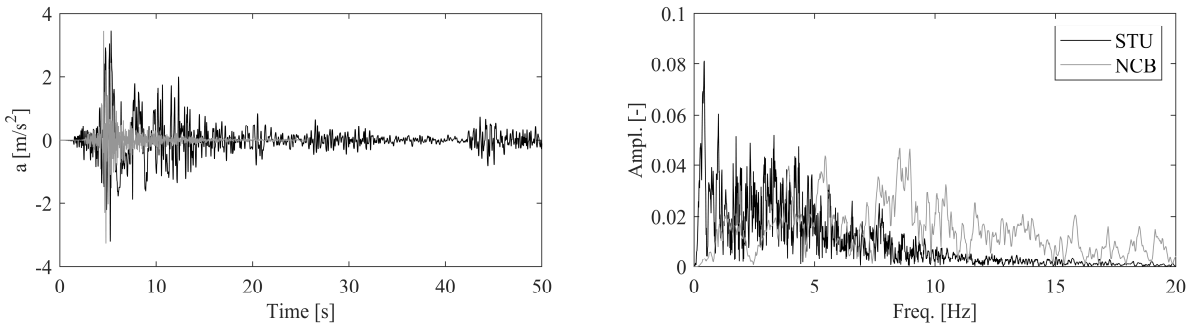

Figure 2: Acceleration time histories and Fourier Spectra of the input motions (scaled at 0.35g).

3.2 Linear analyses results

In Figures 3 and 4 are shown the results of the linear analyses with KIN SP in the case of STU and NCB input motion, respectively. Obviously, in Figures 3 and 4 the mobilized shear modulus (G_{mob}) profiles are equal to the shear modulus at small-strain level profiles shown in Figure 1, as the analyses are linear analyses, thus shear modulus degradation is not considered.

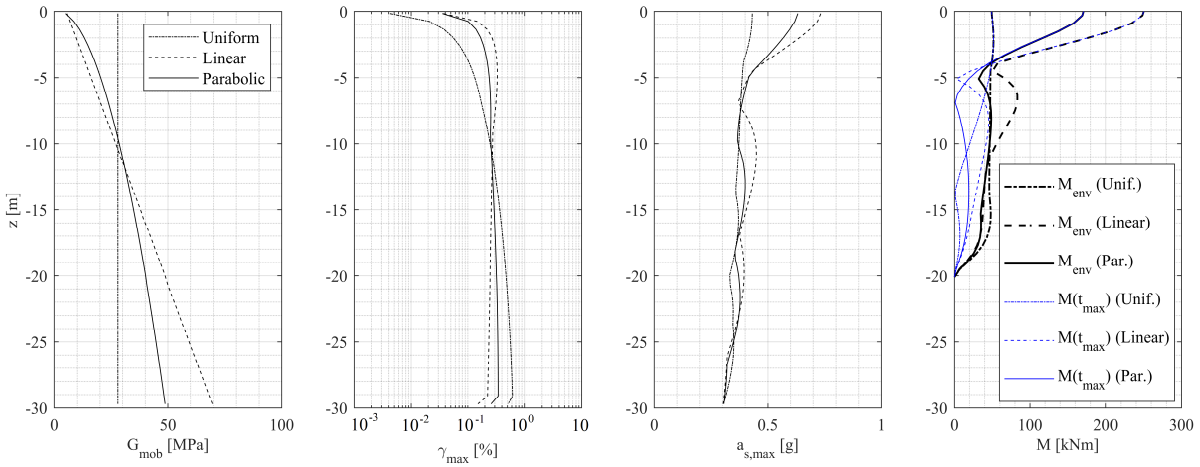

Figure 3: Mobilized shear modulus (G_{mob}), maximum shear strain (γ_{max}), maximum acceleration (a_{max}) profiles, kinematic bending envelope (M_{env}) and bending ($M(t_{max})$) profile at the time when the peak bending at the pile-head is attained for the 3 soil deposits (linear analysis with KIN SP, input motion: STU).

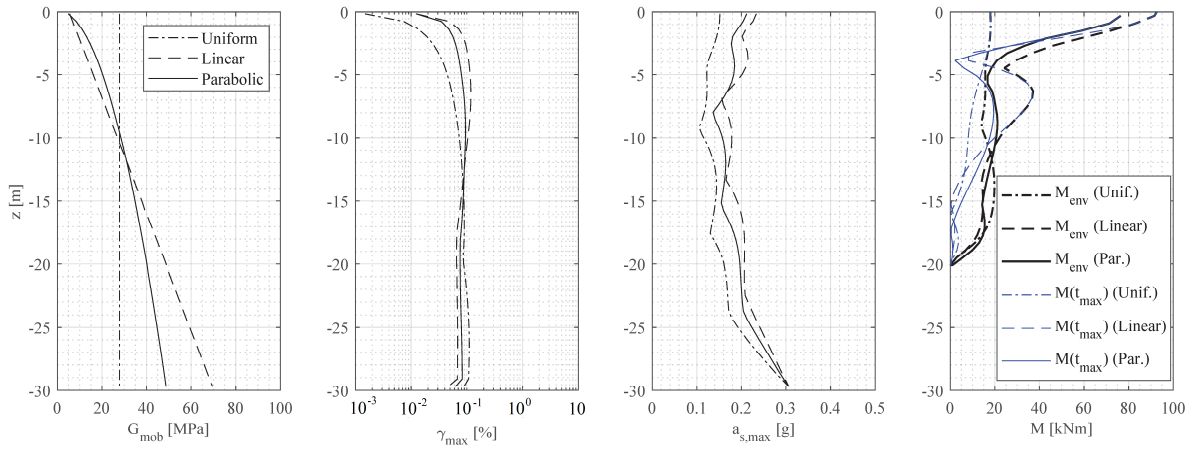

Figure 4: Mobilized shear modulus (G_{mob}), maximum shear strain (γ_{max}), maximum acceleration (a_{max}) profiles, kinematic bending envelope (M_{env}) and bending ($M(t_{max})$) profile at the time when the peak bending at the pile-head is attained for the 3 soil deposits (linear analysis with KIN SP, input motion: NCB).

In Tables 3 and 4 are compared the results obtained with KIN SP (Figures 3 and 4) and those inferred by using the Equation 2 (or the Equation 3) proposed by Di Laora and Rovithis (2014) [15]. In the Equation 2 $G_s(z_{eff})$ is defined according to the Equation 5, while in the Equation 3 $\gamma_s(z_{eff})$ is computed with the Equation 6.

$$G_s\left(z_{eff}\right) = G_{sD} \cdot \left[a + (1-a) \cdot \frac{z_{eff}}{D} \right]^n \tag{5}$$

$$\gamma_s\left(z_{eff}\right) = \frac{a_s \rho_s z_{eff}}{G_{sD}} \cdot \left[a + (1-a) \cdot \frac{z_{eff}}{D} \right]^{-n} \tag{6}$$

Equation 2 and Equation 3 can be used alternatively, nevertheless they both require as fundamental input data the peak acceleration at the ground surface (a_s), that should be defined according to seismic codes or via a seismic response analysis. In Table 3 the results obtained with KIN SP are compared with those by using the Equation 2 (or 3) in which the values of a_s are those inferred by the seismic response analyses performed with KIN SP.

Profile	Input motion	a_s [g] KIN SP	$\gamma_s(z_{eff})$ [%] Eq. 6	M [kNm] Eq. 3	$\gamma_s(z_{eff})$ [%] KIN SP	M [kNm] KIN SP
Uniform	STU	0.427	$4.94\ 10^{-2}$	55.47	$4.60\ 10^{-2}$	49.27
Uniform	NCB	0.149	$1.73\ 10^{-2}$	19.41	$1.61\ 10^{-2}$	18.02
Parabolic	STU	0.62	$1.77\ 10^{-1}$	173.88	$1.66\ 10^{-1}$	170.84
Parabolic	NCB	0.18	$5.27\ 10^{-2}$	51.66	$5.35\ 10^{-2}$	76.47
Linear	STU	0.72	$3.06\ 10^{-1}$	275.76	$3.02\ 10^{-1}$	250.0
Linear	NCB	0.21	$8.77\ 10^{-2}$	79.07	$8.86\ 10^{-2}$	92.64

Table 3: Comparison between KIN SP and Di Laora and Rovithis (2014) [15] method results. In Equation 6 the values of a_s are those inferred by the seismic response analyses with KIN SP

The comparison shows a good agreement between KIN SP and simplified formulas results, thus reflecting the ability of the method proposed by Di Laora and Rovithis (2014) [15] in capturing the physics of the kinematic interaction phenomenon and assessing the kinematic bending at the pile-head in continuously inhomogeneous linear viscoelastic soil deposit resting on a bedrock. In Table 4 the results obtained with KIN SP are compared with those by using the Equation 2 (or 3) in which the value of a_s is that computed by multiplying a_r (peak acceleration of the input motion) with the short period site amplification factor F_s recommended by the EC 8-1 for a Ground Type D (F_s = 1.5).

Profile	Input motion	a_s [g] KIN SP	$\gamma_s(z_{eff})$ [%] KIN SP	M [kNm] KIN SP	a_s [g] EC8-1	$\gamma_s(z_{eff})$ [%] Eq. 6	M [kNm] Eq. 3
Uniform	STU	0.427	$4.60\ 10^{-2}$	49.27	0.53	$6.08\ 10^{-2}$	68.26
Uniform	NCB	0.149	$1.61\ 10^{-2}$	18.02	0.53	$6.08\ 10^{-2}$	68.26
Parabolic	STU	0.62	$1.66\ 10^{-1}$	170.84	0.53	$1.50\ 10^{-1}$	147.20
Parabolic	NCB	0.18	$5.35\ 10^{-2}$	76.47	0.53	$1.50\ 10^{-1}$	147.20
Linear	STU	0.72	$3.02\ 10^{-1}$	250.0	0.53	$2.23\ 10^{-1}$	201.41
Linear	NCB	0.21	$8.86\ 10^{-2}$	92.64	0.53	$2.23\ 10^{-1}$	201.41

Table 4: Comparison between KIN SP and Di Laora and Rovithis (2014) [15] method results. In Equation 6 the values of a_s are those inferred by multiplying a_r (0.35 g) with the site amplification factor (F_s) recommended in EC8-1

As can be observed in Table 4, pile-head kinematic bending predicted with the Equation 3 by using the design peak ground acceleration suggested in EC8-1 (in the Equation 6) can lead both to underestimate or overestimate the kinematic bending. Thus, the use of simplified formulas (Equations 2, 3, 5, 6) without a proper assessment of the peak ground acceleration should be avoided, as in some cases can result less conservative.

4 INFLUENCE OF NONLINEAR SOIL RESPONSE

4.1 Reference soil deposit for nonlinear analyses

Nonlinear analyses have been carried out using the shear modulus at small-strain distributions with depth shown in Figure 1 and employing as soil modulus reduction curve that described in Figure 5.

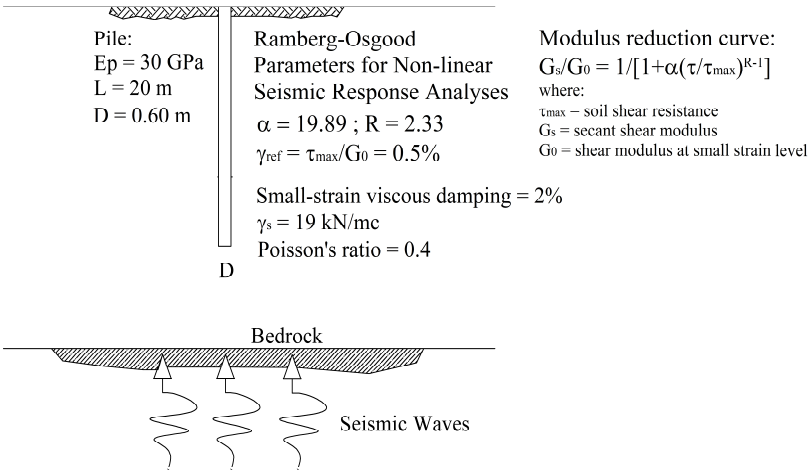

Figure 5: Reference model used for nonlinear kinematic interaction analyses.

KIN SP analyses are preceded by SRAs in the time domain with the code ONDA. In ONDA the nonlinear soil behaviour is modelled using the Ramberg-Osgood constitutive law.

The parameters α, R and γ_{ref} of the Ramberg-Osgood model used in this study are equal to 19.89, 2.33 and 0.5%, respectively. The reference shear strain, γ_{ref}, was used to define the shear strength (τ_{max}) profiles shown in Figure 1 and obtained with the relationship: $\tau_{max}(z)=G_0(z)\gamma_{ref}$. The acceleration time histories (Table 2, Figure 2) have been scaled to values of a_r equal to 0.20g and 0.35g, and applied to the base of the soil deposit model.

4.2 Nonlinear analyses results

In Figures 6 and 7 are show the results obtained considering: a) the three soil shear modulus profiles in Figure 1, b) the nonlinear soil response with the Ramberg-Osgood constitutive model (Figure 5) and applying at the base of the model the STU and NCB input motion, respectively, scaled at 0.20g.

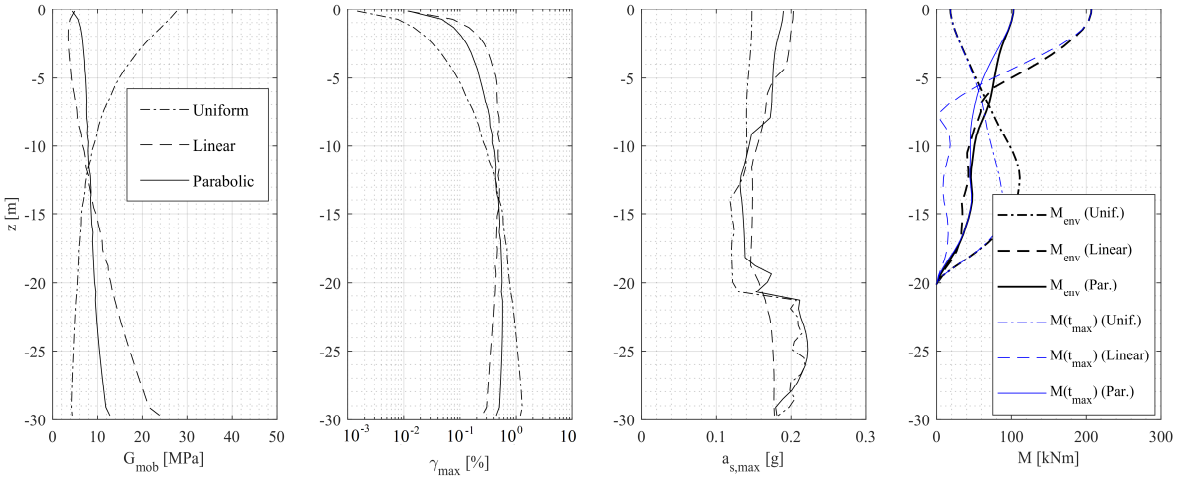

Figure 6: Mobilized shear modulus (G_{mob}), maximum shear strain (γ_{max}), maximum acceleration (a_{max}) profiles, kinematic bending envelope (M_{env}) and bending ($M(t_{max})$) profile at the time when the peak bending at the pile-head is attained for the 3 soil deposits (KIN SP results, input motion: STU scaled at 0.20g).

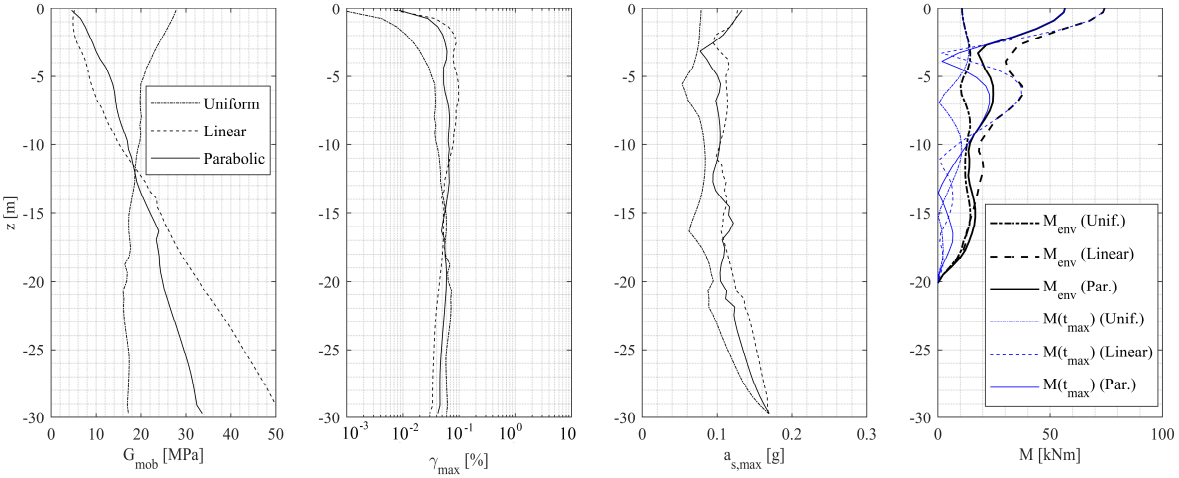

Figure 7: Mobilized shear modulus (G_{mob}), maximum shear strain (γ_{max}), maximum acceleration (a_{max}) profiles, kinematic bending envelope (M_{env}) and bending ($M(t_{max})$) profile at the time when the peak bending at the pile-head is attained for the 3 soil deposits (KIN SP results, input motion: NCB, scaled at 0.20g).

In Figures 8 and 9 are show the results for STU and NCB input motion, respectively, scaled at 0.35g.

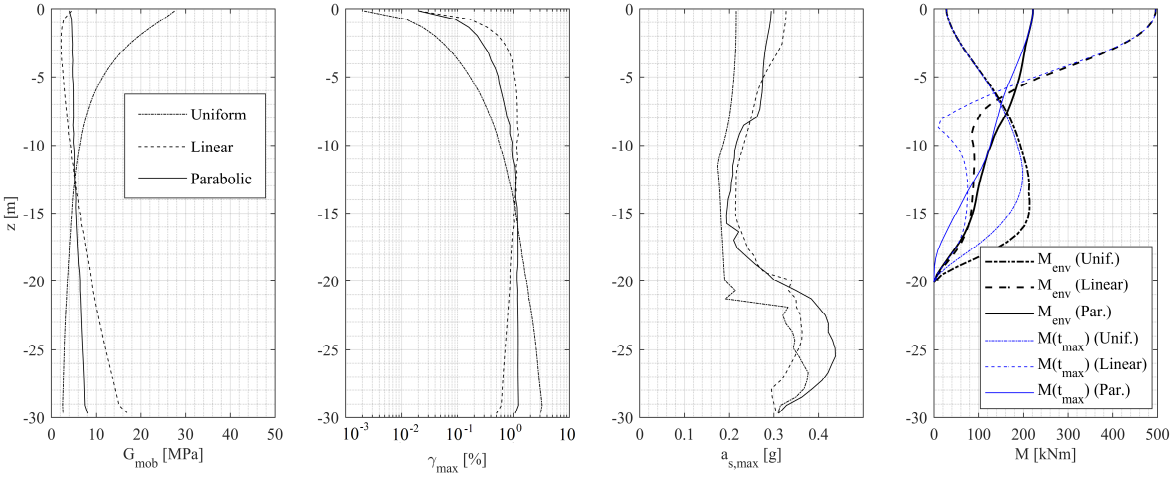

Figure 8: Mobilized shear modulus (G_{mob}), maximum shear strain (γ_{max}), maximum acceleration (a_{max}) profiles, kinematic bending envelope (M_{env}) and bending ($M(t_{max})$) profile at the time when the peak bending at the pile-head is attained for the 3 soil deposits (KIN SP results, input motion: STU scaled at 0.35g).

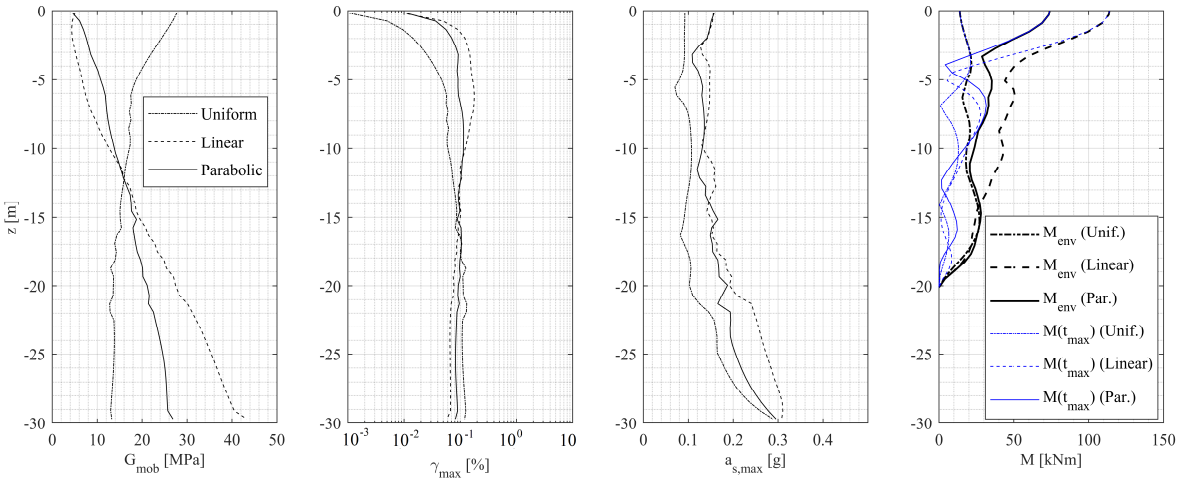

Figure 9: Mobilized shear modulus (G_{mob}), maximum shear strain (γ_{max}), maximum acceleration (a_{max}) profiles, kinematic bending envelope (M_{env}) and bending ($M(t_{max})$) profile at the time when the peak bending at the pile-head is attained for the 3 soil deposits (KIN SP results, input motion: NCB scaled at 0.35g).

In Figure 10 are compared the peak bending moments at the pile-head obtained with KIN SP with those inferred by using the Equation 2 in which the values of a_s are those computed in the nonlinear SRAs with ONDA, and the values of $G_s(z_{eff})$ are the G_{mob} (Figures 6-9) at the z_{eff} depths. The effective depths z_{eff} have been recalculated to consider the soil modulus degradation due to the nonlinear soil response, nevertheless the updated values of z_{eff} are very close to the initial values presented in Table 1.

Despite the comparison shows a good agreement between KIN SP and Equation 2, the results obtained by using the Equation 2 can be computed only if both the $G_s(z_{eff})$ and the a_s values are known. Thus, an a priori assessment of the pile-head kinematic bending via Equation 2 is extremely difficult if the intent is to consider the nonlinear soil response. Indeed, even if the a_s can be defined according to seismic codes and z_{eff} is slightly influenced by soil modulus

degradation, the mobilized shear modulus at the effective depth $G_s(z_{eff})$ can be assessed only performing a SRA. Moreover, as shown in section 3.2 pile-head kinematic bending predicted by using design peak ground acceleration a_s suggested in seismic codes can lead both to underestimate or overestimate the kinematic bending, thus a proper SRA is the most important step in the assessment of pile-head kinematic bending.

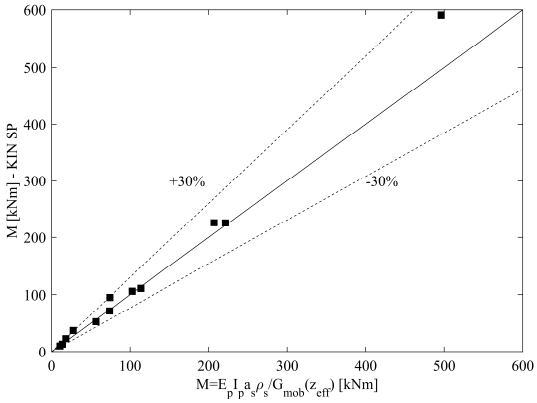

Figure 10: Comparison between the peak bending at the pile-head obtained with KIN SP and Equation 2.

5 INFLUENCE OF PILE CRACKING

In this section are shown some representative results obtained with KIN SP considering the influence of pile cracking. In Figure 11 are shown the bending moment envelopes corresponding to the following conditions: 1) initial shear modulus distribution with depth linear and parabolic (Figure 1), 2) input motion STU scaled at 0.20g and 0.35 g, 3) pile diameter equal to 0.60 m. In the results shown in Figure 11 the nonlinear soil response is considered by using the Ramberg-Osgood model as described in Figure 5.

In the three graphs of Figure 11, the black dashed line represents the bending envelope neglecting the pile nonlinear behaviour, the blue dotted line the bending moment distribution with depth at the time (t_{max}) in which the peak bending at the pile-head is attained neglecting the pile nonlinear behaviour.

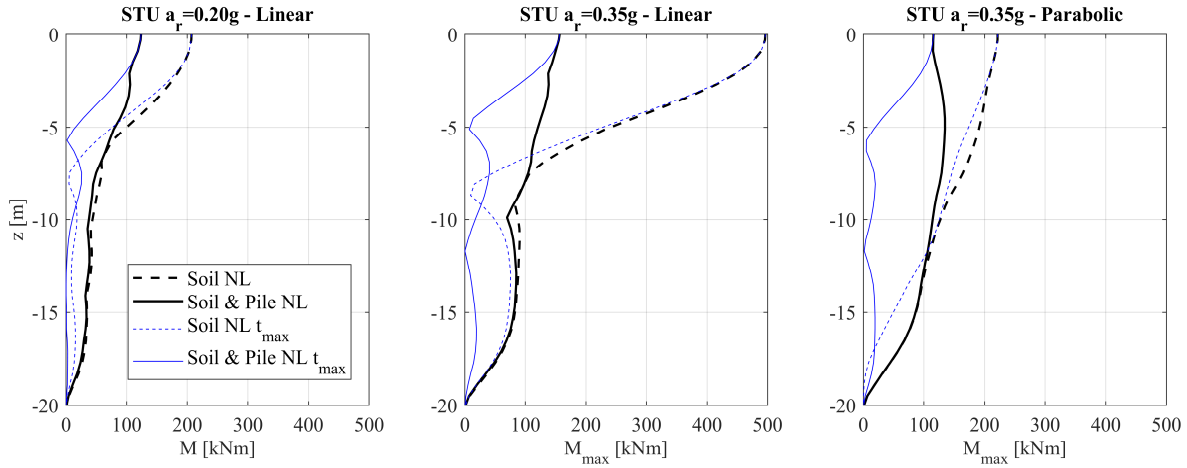

Figure 11: Comparison of bending envelopes w/o considering and considering pile nonlinear behaviour.

The black continuous line and the blue continuous line represent the bending envelope and the bending moment at t_{max}, respectively, obtained considering also the nonlinear pile modelling described in section 2. A steel reinforcement ratio (ρ_s) equal to 1% (14ϕ16) was considered. The cracking bending moment was equal to 96 kNm.

Looking at the results in Figure 11 it can be observed the importance of a more realistic pile modelling after the first cracking of the reinforced concrete sections. The influence of the reinforcement ratio has been studied in Stacul et al. (2019) [18] and its increase leads to an increase of the cracking bending moment and thus to larger bending moments.

In Figure 12 are shown the 'pile bending vs. curvature' and 'pile bending vs. time' graphs, computed with KIN SP, at the pile-head sections for the cases reported in Figure 11.

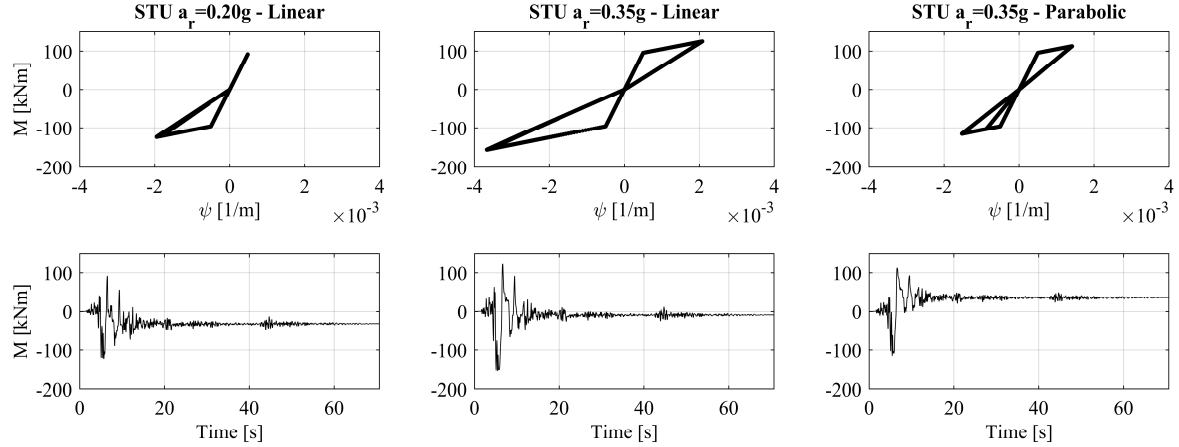

Figure 12: 'Bending vs. Curvature' and 'Bending vs. time' at the pile-head in NL analyses with KIN SP

6 CONCLUDING REMARKS

In this work, the code KIN SP has been used to study the pile-soil kinematic interaction phenomenon. Kinematic analyses have been carried out using as input the SRA analysis results inferred by a SRA-tool (ONDA) merged with KIN SP. Nonlinear soil response has been accounted with the Ramberg-Osgood constitutive model. Moreover, KIN SP has been enhanced to consider the pile post-cracking behavior.

The latter enhancement permitted to properly model the cyclic variation of the pile flexural rigidity after the first cracking and thus to account for the cyclic variation of the pile-soil relative stiffness.

The analyses have been performed on three simplified soil profiles having an initial uniform, linear and parabolic shear modulus distribution with depth and characterized by the same average shear wave velocity of the first 30 m (subsoil type D, according to EN-1998-1). Pile-head kinematic bending obtained with KIN SP has been compared with that inferred by a simplified solution available in literature. This simplified solution is based on the main assumptions that the soil is a linear viscoelastic material and the pile remains in the uncracked stage. Pile and soil nonlinearities have been shown to be relevant in the assessment of the kinematic bending at the pile-head, especially in the case of strong earthquake motions. Moreover, an a priori assessment of the pile-head kinematic bending via simplified solution is extremely difficult if the intent is to consider the soil nonlinear response. In fact, this simpli-

fied solution requires as input the peak acceleration at the ground surface and the mobilized shear modulus at an effective depth (or as an alternative the maximum soil shear strain at an effective depth). Nevertheless, these data can be assessed only performing a nonlinear SRA. The use of simplified solutions with peak-ground acceleration suggested in seismic codes may lead to overestimate or underestimate kinematic bending up to 100 % compared to KIN SP results. Finally, has been shown that the difficulties in the assessment of kinematic bending with simplified formulations increase when also the pile nonlinear response is accounted.

REFERENCES

[1] G.W. Blaney, E. Kausel, J.M. Roesset, Dynamic stiffness of piles. *Proc. 2nd Int. Conf. Num. Methods Geomech. Virginia Polytech. Inst. And State Un. Blacksburg VA II*, 1010-1012, 1976.

[2] R. Dobry, M.J. O'Rourke, Discussion of "Seismic Response Of End-bearing Piles" by Raul Flores-Berrones and Robert V. Whitman (April, 1982). *Journal of Geotechnical Engineering* **109**(5), 778-781, 1983.

[3] R. Flores-Berrones, R.V. Whitman, Seismic response of end-bearing piles. *J. Geotech. Engng. Div., ASCE*, **108**(4), 554-569, 1982.

[4] A.M. Kaynia, E. Kausel, Dynamic stiffness and seismic response of pile groups. Research Report R82-03, Massachussets Inst. Of Technology, 1982.

[5] M. Kavvadas, G. Gazetas, Kinematic seismic response and bending of free-head piles in layered soil. *Geotechnique,* **43**(2), 207-222, 1993.

[6] A. Tabesh, H. Poulos H, Pseudostatic approach for seismic analysis of single piles. *Journal of Geotechnical and Geoenvironmental Engineering,* **127**(9), 757-765, 2001.

[7] G. Mylonakis, Simplified model for seismic pile bending at soil layer interfaces. *Soils and Foundations,* **41**(4), 47-58, 2001.

[8] S. Nikolaou, G. Mylonakis, G. Gazetas, T. Tazoh, Kinematic pile bending during earthquakes: analysis and fields measurements. *Géotechnique,* **51**(5), 425-440, 2001.

[9] R. Di Laora, A. Mandolini, G. Mylonakis, Insight on kinematic bending of flexible piles in layered soil, *Soil Dynamics and Earthquake Engineering,* **43**, 309-322, 2012.

[10] K.J. Bentley, M.H. El Naggar, Numerical analysis of kinematic response of single piles. *Canadian Geotechnical Journal,* **37**(6), 1368-1382, 2000.

[11] R. Di Laora, G. Mylonakis, A. Mandolini, Pile-head kinematic bending in layered soil. *Earthquake Engineering and Structural Dynamics,* **42**(3), 319-337, 2013.

[12] R.M.S. Maiorano, S. Aversa, G. Wu, Effects of soil non-linearity on bending moments in piles due to seismic kinematic interaction. In *Proceedings of the 4th International Conference on Earthquake Geotechnical Engineering*, Thessaloniki, Greece (pp. 25-28), 2007.

[13] G. Wu, W.L. Finn, Dynamic nonlinear analysis of pile foundations using finite element method in the time domain. *Canadian Geotechnical Journal,* **34**(1), 44-52, 1997.

[14] NEHRP, Recommended Provisions for Seismic Regulations for New Buildings and Other Structures. Building Seismic Safety Council, Washington DC, 1997.

[15] R. Di Laora, E. Rovithis, Kinematic bending of fixed-head piles in nonhomogeneous soil. *Journal of Geotechnical and Geoenvironmental Engineering*, **141**(4), 04014126, 2014.

[16] R. Di Laora, G. Mylonakis, A. Mandolini, Size limitations for piles in seismic regions. *Earthquake Spectra*, **33**(2), 729-756, 2017.

[17] G. Mylonakis, R. Di Laora, A. Mandolini, The role of pile diameter on earthquake-induced bending. In *Perspectives on European Earthquake Engineering and Seismology* (pp. 533-556). Springer, Cham, 2014.

[18] S. Stacul, A. Franceschi, N. Squeglia, Effect of non-linear soil response and pile post-cracking behavior on seismically induced bending moments in fixed-head long piles. In *7th International Conference on Earthquake Geotechnical Engineering,* Rome, 17-20 June 2019.

[19] S. Stacul, N. Squeglia, KIN SP: A boundary element method based code for single pile kinematic bending in layered soil. *Journal of Rock Mechanics and Geotechnical Engineering,* **10**(1), 176-187, 2018.

[20] D.C.F. Lo Presti, C. Lai, I. Puci, ONDA: Computer Code for Nonlinear Seismic Response Analyses of Soil Deposits. *Journal of Geotechnical and Geoenvironmental Engineering,* Vol. **132**(2), 223-236, 2006.

[21] A. Angina, A. Steri, S. Stacul, D. Lo Presti, Free-Field Seismic Response Analysis: The Piazza dei Miracoli in Pisa Case Study. *International Journal of Geotechnical Earthquake Engineering (IJGEE)*, **9**(1), 1-21, 2018.

[22] G. Fiorentino, C. Nuti, N. Squeglia, D. Lavorato, S. Stacul, One-dimensional nonlinear seismic response analysis using strength-controlled constitutive models: The case of the leaning tower of Pisa's subsoil. *Geosciences*, **8**(7), 228, 2018.

[23] W. Ramberg, W.R. Osgood, Description of Stress-Strain Curves by Three Parameters; National Advisory Committee for Aeronautics: Washington, DC, USA, 1943.

[24] S. Stacul, N. Squeglia, Analysis Method for Laterally Loaded Pile Groups Using an Advanced Modeling of Reinforced Concrete Sections. *Materials*, **11**(2), 300, 2018.

[25] S. Stacul, N. Squeglia, F. Morelli, Laterally Loaded Single Pile Response Considering the Influence of Suction and Non-Linear Behaviour of Reinforced Concrete Sections. *Applied Sciences*, **7**(12), 1310, 2017.

[26] G. Andreotti, C.G. Lai, A nonlinear constitutive model for beam elements with cyclic degradation and damage assessment for advanced dynamic analyses of geotechnical problems. Part I: theoretical formulation. *Bulletin of Earthquake Engineering,* 1-17, 2017.

[27] EN-1998-1. Eurocode 8: Design of structures for earthquake resistance-Part 1: General rules, seismic actions and rules for buildings, 2005.

[28] L. Luzi, F. Pacor, R. Puglia, Italian Accelerometric Archive v 2.1. *Istituto Nazionale di Geofisica e Vulcanologia, Dipartimento della Protezione Civile Nazionale,* doi: 10.13127/ITACA/2.1, 2016.

[29] E.M. Rathje, N.A. Abrahamson, J.D. Bray, Simplified frequency content estimates of earthquake ground motions. *Journal of Geotechnical and Geoenvironmental Engineering*, **124**(2), 150-159, 1998.